A 4×4 Logarithmic Spike Timing Encoding Scheme for Olfactory Sensor Applications

Bin Guo[1], Amine Bermak[1], Maxime Ambard[2], Dominique Martinez[2]
[1]Electronic and Computer Engineering Department, Hong Kong University of Science and Technology
Clear Water Bay, Kowloon, Hong Kong. Email: guobin@ust.hk
[2]CORTEX Group, LORIA-INRIA, Nancy, France. Email: ambard@loria.fr

***Abstract*— This paper presents a 4×4 logarithmic spike-timing encoding scheme used to translate the output of an integrated tin oxide gas sensor array into spike sequence, which is exploited to perform gas recognition. Hydrogen, Ethanol and Carbon monoxide were used to characterize the gas sensor array. The collected data were then used to test the proposed circuit for spike encoding and gas recognition. Simulation results illustrate that a particular analyte gas generates a unique spike pattern with certain spike ordering sequence, which is independent of the gas concentration. This unique spike sequence can thus be used to recognize different gases. In addition, the concentration information can also be extracted from the time-to-the-first spike in the sequence making it possible to perform not only gas/odor recognition but quantification as well.**

Keywords: Logarithmic Spike Timing, Tin Oxide, Gas Sensor Array, Spike Sequence

I. Introduction

BIOLOGICAL neurons communicate using short and sudden increases in their membrane voltage, which are more commonly known as action potentials or spikes. Recent research has shown that neurons encode information in spikes not only with firing frequency, but also more effectively with precise timing of single spikes [1]. Spike timing seems to be the basis for some neural computations, such as auditory neurons in cochlear ganglion and auditory brain system nuclei [2], ganglion cells in retina [3] and cells of rat barrel cortex [4]. Stimuli with temporal structures can thus drive different neurons to spike as spatiotemporal codes for such stimuli. Temporally stable stimuli can also be transformed into spatiotemporal codes. For instance, different odors evolve particular spatiotemporal spikes of the projection cells in the locust antennal lobe [5]. Such spatiotemporal spike patterns from a population of neurons can be simply encoded as rank orders [6] with rapid and robust processing, where only one spike per neuron is used and the interconnections between individual neurons are not needed. The generated spike trains can be recognized using neural networks or state machines in digital systems [7].

Recent electrophysiological recordings in the mouse olfactory bulbs have shown that the phase of the firing of a principal neuron relative to the beginning of each respiratory cycle reflects input intensity [8]. In addition, these experimental results and theoretical work reported in [1] show an approximate logarithmic relationship between firing latency and odor intensity. In this paper, we propose an integrate-and-fire type of neuron [9], which can convert the outputs of a tin oxide gas sensor into logarithmic spike timings. A 4×4 logarithmic spike-timing encoding circuit is designed and simulated with the experimentally obtained data from an integrated tin oxide gas sensor array. The sensor array consists of 4×4 gas sensors with micro-hotplate (MHP) structures using surface micromachining process suitable for large dimension integrated arrays [10], [11], [12].

The remainder of the paper is organized as follows. Section II describes the principle and the characterization of the gas sensor array. Section III reports the gas recognition algorithm and the design of the encoding circuit. Section IV illustrates the simulation results while section V concludes the paper.

II. Sensor array characterization

The monolithic 4×4 tin oxide gas sensor array was designed and fabricated using our in-house 5 μm 1-metal, 1-poly CMOS process. The top view of the fabricated sensor element with the micro heater and the electrodes is shown in Figure 1.

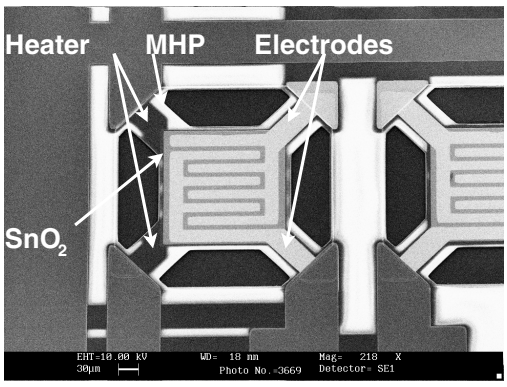

Fig. 1. The SEM picture of the sensor element.

The MHP is at the center of the sensor element and has a dimension of 190×190 μm^2. A 2.8 μm air gap between the hotplate membrane and the SiO_2 underneath the membrane is formed by etching a sacrificial polysilicon layer. The SnO_2 sensing film is deposited onto the MHP using a sputtering method. The sensor signal is measured from the resistance variation across the two Pt electrodes. Different post-treatment combinations were performed on the sensors within the array, including metal catalysts (Pt, Pd and Au) in 3 columns and

ion implantations (B, P and H) in 3 rows, which results in a response variation across the 16 sensors. The fabricated gas sensor array was characterized using 3 different analyte gases: Hydrogen, Ethanol and Carbon monoxide. All the tests were done at an operating temperature of 300 ^{o}C. The sensitivity is used as the extracted feature, which is defined as $\frac{R_s}{R_0}$, where R_0 and R_s represent the baseline resistance and the resistance when the sensor is exposed to analyte gases, respectively. R_0 is measured when the sensor is exposed to dry air. For relatively high concentrations, the sensitivity of the sensors to different gases is described in Eq. (1) and (2).

$$\frac{(R_s)_{ij}}{(R_0)_{ij}} = \alpha_{ij} C_j^{r_{ij}}, \quad j = 1; \tag{1}$$

$$\frac{(R_s)_{ij}}{(R_0)_{ij}} = \alpha_{ij} e^{r_{ij} \cdot C_j}, \quad j = 2, 3. \tag{2}$$

Where i (equals to 1 - 16) represents the i^{th} sensor in the sensor array and j (equals to 1, 2 or 3) represents the tested gases namely: Hydrogen, Ethanol and Carbon monoxide, respectively. C is the gas concentration. Besides a power law [13] response to Hydrogen, the sensor array shows an exponential law relationship to Ethanol and Carbon monoxide. The two parameters α and r are coefficients which can be extracted by fitting the experimental curves of the sensor's outputs. A new parameter a is defined as $a_{ij} = \frac{r_{ij}}{\min(r_{ij})}$, which will be used in the logarithmic spike-timing circuits, where $\min(r_{ij})$ is the minimum over i, hence for a fixed j (given gas), $\min(r_{ij})$ equals to the smallest r_{ij} among the 16 sensors. By measuring the sensitivity at different gas concentrations, the coefficient r_{ij} and α_{ij} can be calculated from the fitting of the sensitivity-to-concentration curves using Eq. (1) and (2). The baseline resistance R_0 for different sensors and a_{ij} for different type of gases are listed in Table I.

TABLE I

GAS SENSOR ARRAY CHARACTERIZATION RESULT. THE TOP QUADRANT OF THE TABLE SHOWS THE BASELINE RESISTANCE FOR EACH SENSOR WITHIN THE ARRAY. THE REMAINING THREE QUADRANTS REPRESENT THE a_{ij} FOR EACH TESTED GASES.

R_0 (KΩ)	Col1	Col2	Col3	Col4
Row1	22.3	240	26.95	17.08
Row2	24.94	117.88	16.81	13.37
Row3	22.61	233.9	16.59	18.14
Row4	23.47	155.02	29.37	19.85
a_{i1} (Hydrogen)	Col1	Col2	Col3	Col4
Row1	1.001	2.506	2.338	1.658
Row2	1.000	1.641	2.220	1.600
Row3	1.193	2.506	2.475	1.847
Row4	1.225	1.961	2.149	1.886
a_{i2} (Ethanol)	Col1	Col2	Col3	Col4
Row1	1.558	6.674	1.139	1.000
Row2	1.302	6.233	1.000	1.093
Row3	2.535	6.674	1.116	1.209
Row4	2.651	6.488	1.116	1.279
a_{i3} (CO)	Col1	Col2	Col3	Col4
Row1	1.000	2.778	2.111	1.667
Row2	1.444	2.055	1.389	1.555
Row3	1.278	2.778	1.389	1.778
Row4	1.722	2.389	2.222	1.889

III. LOG-SPIKE-TIMING NEURON AND GAS RECOGNITION ALGORITHM

The circuit shown in Figure 2.a is used to transform the resistance R_s of the sensor to voltage outputs featuring a logarithmic relationship with respect to the resistance. Using V_r as a reference voltage, R_s is converted into V_s using the logarithmic readout circuit of Figure 2.a, where a Base-Collector shorted bipolar transistor is used to generate the logarithmic voltage output from R_s. I_0 is a current generated by the baseline resistance R_0, using the same method (with a different reference voltage) in the calibration stage. By setting proper current mirror ratios, $V_s < V_0$ can be ensured, which validates the spiking neuron circuit. Figure 2.b shows the spiking neuron circuit. When the clock signal clk is high, the membrane voltage V_m is set to V_s by transistor M_1. When the clock transits to low, the membrane voltage begins to integrate until it reaches V_0, with a slope set by I_E. When V_m = V_0, the comparator triggers and the voltage V_m increases sharply since M_2 is turned on. At the same time a spike is generated at the output. The membrane voltage is then reset by transistor M_3. The width of the spike is determined by the current in M_{11}, which is set by the bias voltage V_p, and the value of capacitor C_1.

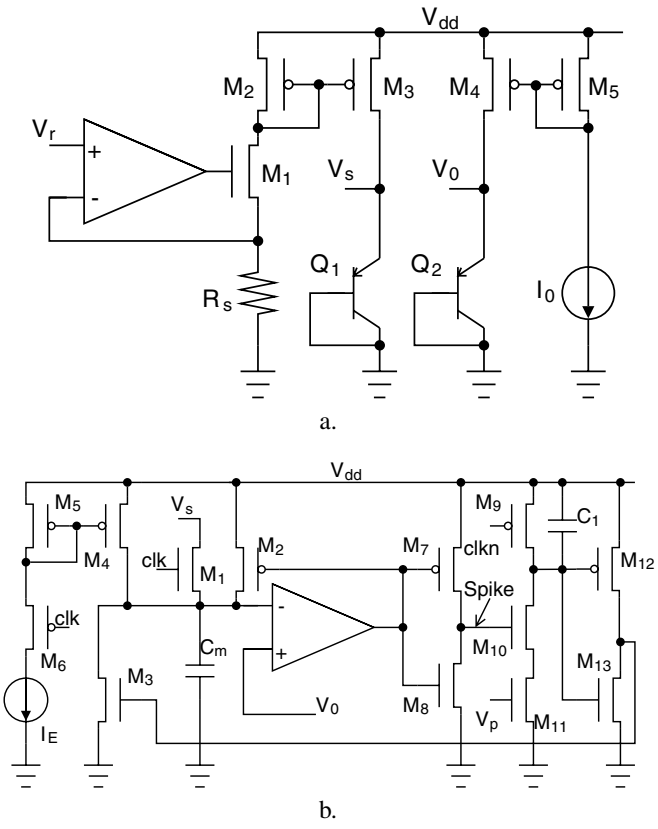

Fig. 2. (a) The resistance to log-output circuit. (b) The integrate and fire (spiking) neuron.

From Figure 2, the equation for the logarithmic spike timing delay is given as:

$$I_E \cdot \Delta T_{ij} = B + A \ln[\frac{(R_s)_{ij}}{(R_0)_{ij}}] \quad (3)$$

where ΔT_{ij} is the timing delay for a neuron to generate a spike after the integration starts, or the time-to-the-first-spike (TFS). A and B are constants determined by the circuit parameters and are the same for all the neurons.

By setting I_E according to the value of a_{ij}, Eq. (3) can be rewritten as:

$$a_{ij} \cdot \Delta T_{ij} = B + A \ln[\frac{(R_s)_{ij}}{(R_0)_{ij}}] \quad (4)$$

where a_{ij} is the parameter with values listed in Table 1. The use of a_{ij} coefficients instead of r_{ij} in Eq. (4) is selected because of the wide dynamic range of r_{ij}, i.e. $r_{i1} \rightarrow$ (0.0043 - 0.0287), $r_{i2} \rightarrow$ (0.972 - 2.436) and $r_{i3} \rightarrow$ (0.0018 - 0.005). So with different j, a 10-bit current source should be used to cover the 3 decades variation. Similarly, with different i, at least 8-bit should be used for the sake of computation accuracy. Thus a current source with 18-bit is required, which is hard to implement. However, using a_{ij}, with a range of (1 - 6.674) shown in Table I, a 10-bit current source is sufficient. Combining Eq. (1) and (2) with Eq. (4) we can write:

$$\begin{aligned} \Delta T_{ij} &= B \cdot \tfrac{\min(r_{ij})}{r_{ij}} + A \cdot \tfrac{\min(r_{ij})}{r_{ij}} \cdot \ln \alpha_{ij} \\ &+ A \cdot \min(r_{ij}) \ln C_j, \quad j = 1; \end{aligned} \quad (5)$$

$$\begin{aligned} \Delta T_{ij} &= B \cdot \tfrac{\min(r_{ij})}{r_{ij}} + A \cdot \tfrac{\min(r_{ij})}{r_{ij}} \cdot \ln \alpha_{ij} \\ &+ A \cdot \min(r_{ij}) \cdot C_j, \quad j = 2, 3. \end{aligned} \quad (6)$$

It should be noted that j = 1, 2 or 3, correspond to Hydrogen, Ethanol and Carbon monoxide, respectively. Thus for each gas, we can compute the relative position (interval) of two neighboring spikes in the 16-spike sequence as:

$$\begin{aligned} \Delta T_{ij} - \Delta T_{qj} &= B \cdot \tfrac{\min(r_{ij})}{r_{ij}} + A \cdot \tfrac{\min(r_{ij})}{r_{ij}} \cdot \ln \alpha_{ij} \\ &- (B \cdot \tfrac{\min(r_{ij})}{r_{qj}} + A \cdot \tfrac{\min(r_{ij})}{r_{qj}} \cdot \ln \alpha_{qj}) \end{aligned} \quad (7)$$

Where q and j represent two individual neurons and $\min(r_{ij}) = \min(r_{qj})$. Eq. (7) indicates that the relative position of the spike is unique for each gas and independent of the gas concentration. This very interesting feature can be used to perform efficient gas recognition.

IV. Results and discussion

The logarithmic spike-timing encoding circuit was designed using ALCATEL 0.35 μm CMOS process and simulated using CADENCE Spectre. The current I_0 and I_E were simulated using ideal sources, where $a_{ij} = 1$ corresponds to $I_E = 1$ nA. Figure 3.a and b illustrate the simulated outputs of the circuit shown in Figure 2.a and b, respectively. Figure 3.a shows that a resistance input is converted to voltage output in a logarithmic relationship. Figure 3.b shows simulation results of the clock signal, the neuron membrane voltage V_m and the spike output of the logarithmic spike timing neuron, illustrated in Figure 2.b. Initially, when the clock is high, the membrane voltage is set to V_s. When the clock signal is switched low (at about 2 ms), the membrane voltage begins to integrate. The slope of the integration curve is determined by I_E in Figure 2.b. When V_m reaches V_0, a spike is generated at the output (the $spike$ node in Figure 2.b). The spike lasts for about 150 ns. The integration and spike process is repeated with a period of 5 ms.

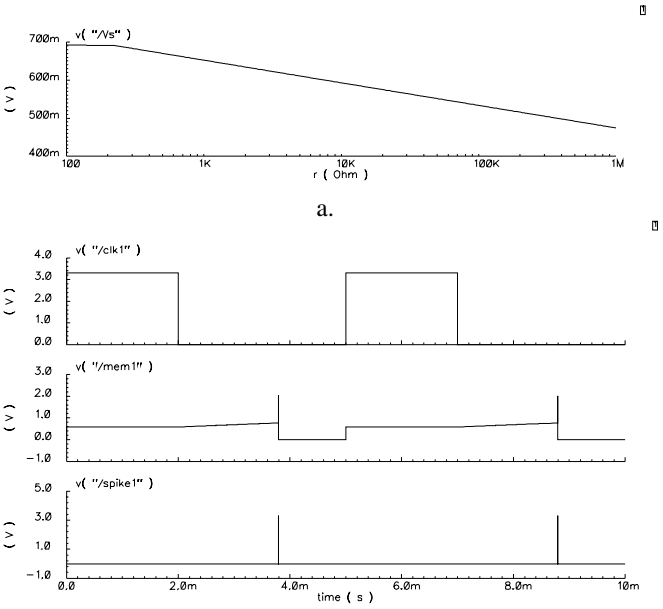

Fig. 3. (a) Response of the resistance to log-output circuit. (b) Spiking neuron circuit simulation result. Waveforms from top to bottom are the control signal, the neuron membrane voltage and the spike output, respectively.

Figure 4 - 6 illustrate the encoding circuit responses to different gases with different concentrations. It should be noted that the circuit was tested with real gas sensor data. Each neuron in the 4×4 encoding circuit uses R_s and R_0 corresponding to a given sensor in the integrated sensor array. Different values of I_E are set according to a_{ij} listed in Table I for different gases to validate the algorithm described in section III. As shown in Figure 4, when the target gas is Hydrogen, the 10^{th} neuron generates the first spike. The 16 spikes are labelled and a unique sequence is obtained. The sequence is insensitive to changes in gas concentration. The same experiment was repeated for Ethanol and Carbon monoxide. Figure 5 and 6 show different spiking sequences from Hydrogen. In each case, when the gas concentration increases, the time delay to the first spike in the sequence decreases. The spike sequence (the relative position) and spike patten (the time interval of neighboring spikes) are again insensitive to changes in gas concentration. Each gas generates a unique spike sequence which can be used to discriminate between different gases. The concentration information is encoded in TFS information.

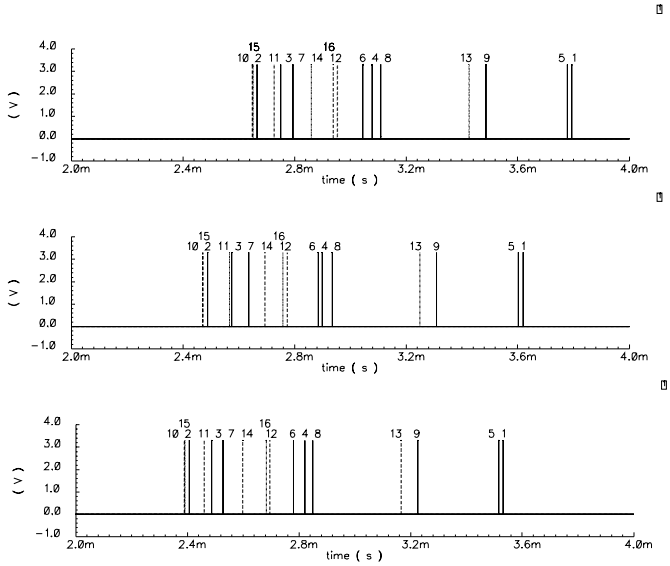

Fig. 4. Circuit's response to Hydrogen at 25 PPM , 50 PPM and 75 PPM, from top to bottom. The TFS is 0.648 ms, 0.471 ms and 0.389 ms, respectively.

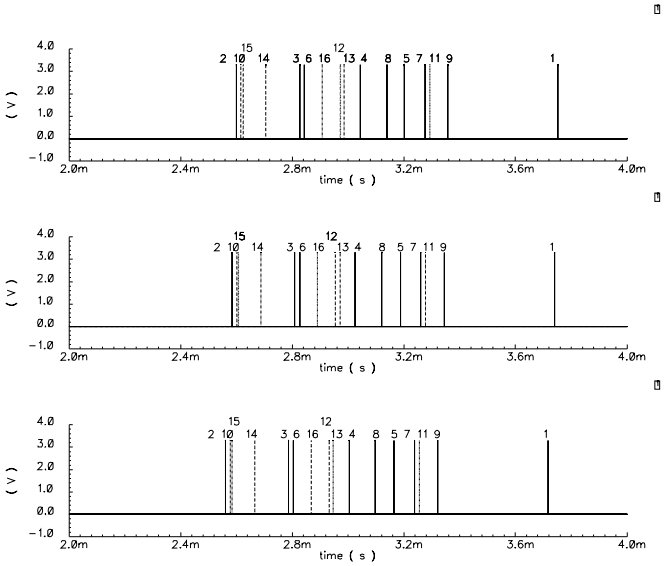

Fig. 6. Circuit's response to Carbon monoxide at 50 PPM, 100 PPM and 150 PPM, from top to bottom. The TFS is 0.599 ms, 0.584 ms and 0.56 ms, respectively.

V. Conclusion

A 4×4 logarithmic spike-timing encoding circuit is designed and simulated in this paper. Tested with real data from an integrated tin oxide gas sensor array, this encoding circuit can generate unique spike sequence for different analyte gases. The unique spike sequence is independent of the gas concentration, thus can be used to discriminate between different gases. Using a relatively simple structure, this encoding scheme illustrates powerful computation capabilities.

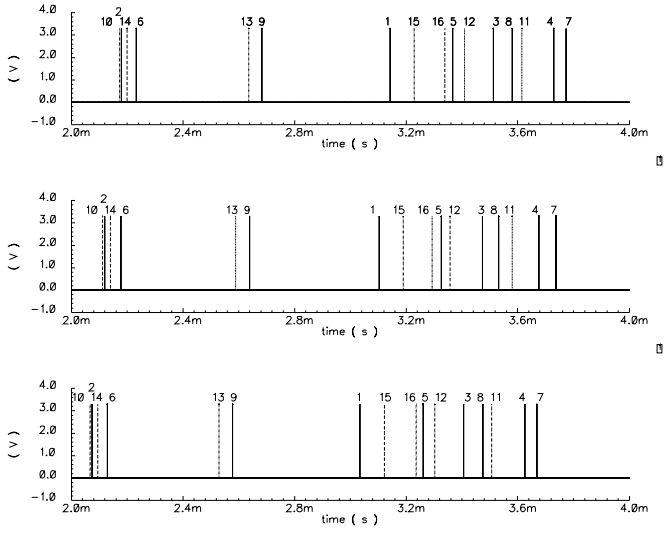

Fig. 5. Circuit's response to Ethanol at 50 PPM, 100 PPM and 150 PPM, from top to bottom. The TFS is 0.173 ms, 0.111 ms and 0.067 ms, respectively.

Acknowledgments

This work was sponsored by (HKUST 6162/04E) from the Research Grant Council of Hong Kong. The authors would like to acknowledge Prof. Gui-Zhen Yan and Prof. Philip Chan for their considerable help on the gas sensor array integration.

References

[1] J. Hopfield, "Pattern Recognition Computation Using Action Potential Timing for Stimulus Representation", Nature, 376, 1995, pp. 33-36.

[2] L. O. Trussell, "Synaptic Mechanisms for Coding Timing in Auditory Neurons", Annual Review of Physiology, 61, 1999, pp. 477-496.

[3] M. J. Berry, D. K. Warland and M. Meister, "The Structure and Precision of Retinal Spike Trains", Proceedings of the National Academy of Sciences of the United States of America, 94, 1997, pp. 5411-5416.

[4] S. Shimegi, T. Akasaki, T. Ichikawa and H. Sato, "Physiological and Anatomical Organization of Multiwhisker Response Interactions in the Barrel Cortex of Rats", Journal of Neuroscience, 20 (16), 2000, pp. 6241-6248.

[5] M. Stopfer and G. Laurent, "Short-term Memory in Olfactory Network Dynamics", Nature (london), 402 (6762), 1999, pp. 664-668.

[6] V. Rullen and S. J. Thorpe, "Rate Coding Versus Temporal Order Coding: What the Retinal Ganglion Cells Tell the Visual Cotex", Neural Computation, 13, 2001, pp. 1255-1283.

[7] D. Z. Jin, "Spiking Neural Network for Recognizing Spatiotemporal Sequences of Spikes", Physical Review E, 69, 2004, pp. 021905.1-13.

[8] T. Margrie and A. Schaefer, "Theta Oscillation Coupled Spike Latencies Yield Computational Vigour in a Mammalian Sensory System", Journal of Physiology, 546, 2003, pp. 363-374.

[9] W. Gerstner and W. M. Kistler, *Spiking neuron models: single neurons, populations, plasticity*, Cambridge University Press,Cambridge 2002.

[10] M. Y. Afridi, J. S. Suehle, M. E. Zaghloul, D. W. Brning, A. R. Hefner, R. E. Cavicchi et al., "A Monolithic CMOS Microhotplate-Based Gas Sensor System", IEEE Sensors Journal, 2 (6), 2002, pp. 644-655.

[11] C. Cane, I. Gracia, A. Gotz, L. Fonseca, E. Lora-Tamayo, M. C. Horrillo, I. Sayago, J. I. Robla, J. Rodrigo and J. Gutierrez, "Detection of Gases with Arrays of Micromachined Tin Oxide Gas Sensors", Sensors and Actuators B, 65, 2000, pp. 244-246.

[12] U. Frey, M. Graf, S. Taschini, K.-U. Kirstein, C. Hagleitner, A. Hierlemann, and H. Baltes, "A Digital CMOS Micro-Hotplate Array for Analysis of Environmentally Relevant Gases", ESSCIRC 2004, Sep 2004, pp. 299-302.

[13] D. Martinez, O. Rochel and E. Hugues, "A Biomimetic Robot for Tracking Specific Odors in Turbulent Plumes", Autonomous Robot, Special Issue on Mobile Robot Olfaction, 20 (3), 2006, pp. 185-195.